Helicity conservation under quantum reconnection of vortex rings

Simone Zuccher*
Department of Computer Science, U. Verona, Ca' Vignal 2, Strada Le Grazie 15, 37134 Verona, Italy

Renzo L. Ricca†
Department of Mathematics & Applications, U. Milano-Bicocca, Via Cozzi 55, 20125 Milano, Italy

(Dated: June 2, 2016)

Here we show that under quantum reconnection, simulated by using the three-dimensional Gross-Pitaevskii equation, self-helicity of a system of two interacting vortex rings remains conserved. By resolving the fine structure of the vortex cores, we demonstrate that total length of the vortex system reaches a maximum at the reconnection time, while both writhe helicity and twist helicity remain separately unchanged throughout the process. Self-helicity is computed by two independent methods, and topological information is based on the extraction and analysis of geometric quantities such as writhe, total torsion and intrinsic twist of the reconnecting vortex rings.

PACS numbers: 47.32.C- (vortex dynamics), 47.32.cf (vortex reconnection and rings), 67.30.he (vortices in superfluid helium), 03.75.Lm (vortices in Bose Einstein condensates), 47.37.+q (hydrodynamic aspects of superfluidity), 02.40.Pc (topology),

arXiv:1606.00366v1 [physics.flu-dyn] 19 Sep 2015

I. INTRODUCTION

Background.—Reconnection of coherent structures play a fundamental rôle in many areas of science. Examples include vortices in classical fluid flows [1, 2], quantum vortex filaments in superfluid Helium [3, 4], magnetic flux tubes in plasma physics [5, 6], phase transitions in mesoscopic physics [7], macromolecules in DNA biology [8]. Here we focus on a single reconnection event, that characterizes superfluid quantum turbulence [9, 10], by analyzing dynamical, geometric and topological properties that are relevant also in classical viscous fluids [2], where similar features such as time asymmetry [4], helicity transfers, randomization of the velocity field and energy cascades [11] are important.

In recent months a number of remarkable results based on experimental observations [12], mathematical analysis [13] and theoretical and numerical work [14] have provided contradictory information as regards helicity transfer through reconnection. On one hand laboratory experiments on the production and evolution of vortex knots in water show [12] that the centerline helicity of a vortex filament remains essentially conserved throughout the spontaneous reconnection of the interacting vortices. This result is mirrored by the mathematical analysis of conservation of writhe and total torsion (for definitions, see Sec.III here below) under the assumption of antiparallel reconnection of the interacting strands [13]. On the other hand recent numerical results [14], based on a linearized model of interacting Burgers-type vortices brought together by an ambient irrotational strain field, show that the initial helicity associated with the skewed geometry is eliminated during the process. This apparent contradiction motivates further the present study.

In this paper we carry out a simulation of the interaction and reconnection of a single pair of identical quantum vortex rings. The evolution is governed by the three-dimensional Gross-Pitaevskii equation (GPE), with the aim to reproduce and analyze in the GPE context the fine details of the prototype reconnection event as studied in [14]. By resolving the fine structure of the vortex cores, we monitor all the relevant dynamical, geometric and topological features of the reconnection process. Consistently with current simulations (see, for example [11]), the peak in the normalized total length of the vortex system, given by an initial stretching process followed by its marked decay, is taken as signature of the reconnection event, providing a precise benchmark for the diagnostics of the mathematical and physical properties associated with the reconnection event.

Governing equations.—Direct numerical simulation of the reconnecting quantum vortex rings is done by using the 3D Gross-Pitaevskii equation (GPE)

$$\frac{\partial\psi}{\partial t} = \frac{\mathrm{i}}{2}\boldsymbol{\nabla}^2\psi + \frac{\mathrm{i}}{2}(1-|\psi|^2)\psi \ , \tag{1}$$

with background density $\rho_b = 1$. Through the Madelung transformation $\psi = \sqrt{\rho}\exp(\mathrm{i}\theta)$, eq. (1) admits decomposition into two equations that can be interpreted in classical fluid dynamical terms, i.e. the continuity equation and the momentum equation, given by

$$\frac{\partial\rho}{\partial t} + \frac{\partial(\rho u_j)}{\partial x_j} = 0 \ , \tag{2}$$

$$\rho\left(\frac{\partial u_i}{\partial t} + u_j\frac{\partial u_i}{\partial u_j}\right) = -\frac{\partial p}{\partial x_i} + \frac{\partial\tau_{ij}}{\partial x_j} \ , \tag{3}$$

where $\rho = |\psi|^2$ denotes fluid density, $\boldsymbol{u} = \boldsymbol{\nabla}\theta$ velocity, $p = \frac{\rho^2}{4}$ pressure, and $\tau_{ij} = \frac{1}{4}\rho\frac{\partial^2\ln\rho}{\partial x_i\partial x_j}$ the so-called quantum stress ($i,j = 1,2,3$). Defects in the wave function ψ represent infinitesimally thin vortices of constant circulation $\Gamma = \oint \boldsymbol{u}\cdot\mathrm{d}\boldsymbol{s} = 2\pi$ of healing length $\xi = 1$.

* simone.zuccher@univr.it
† renzo.ricca@unimib.it

It is well known that GPE conserves mass, given by $M = \int |\psi|^2 \, \mathrm{d}\boldsymbol{x}^3$, and the hamiltonian $E = K + I$, where

$$K = \frac{1}{2} \int \boldsymbol{\nabla}\psi \cdot \boldsymbol{\nabla}\psi^* \, \mathrm{d}\boldsymbol{x}^3 \ , \ I = \frac{1}{4} \int (1 - |\psi|^2)^2 \, \mathrm{d}\boldsymbol{x}^3 \ , \quad (4)$$

denote respectively the kinetic (K) and interaction (I) energy of the system (ψ^* being the complex conjugate of ψ). The term τ_{ij}, negligible compared to the pressure term at length scales much larger than the healing length $\xi = 1$, is expected to be key to vortex reconnection [4], and at scales larger than the vortex core, GPE in the form of eqs. (2) and (3) reduces to the classical compressible Euler equations.

Helicity and self-linking number.—A fundamental quantity of topological fluid mechanics is kinetic helicity, defined by [15]

$$H = \int \boldsymbol{u} \cdot \boldsymbol{\omega} \, \mathrm{d}\boldsymbol{x}^3 \ , \quad (5)$$

where $\boldsymbol{\omega} = \nabla \times \boldsymbol{u}$ is vorticity and the integral is extended over the vorticity volume. H is known to be an invariant of ideal fluid flows and in ideal conditions it admits a topological interpretation in terms of linking number [16]. For a pair of linked vortex rings V_1 and V_2, centred respectively on curves C_1 and C_2 and of equal circulation Γ, eq. (5) can be written as [17, 18]

$$H(V_1, V_2) = \Gamma^2 [SL(V_1) + SL(V_2) + 2Lk(C_1, C_2)] \ , \quad (6)$$

where $H(V_1, V_2)$ is the total helicity of the system, $SL(V_i)$ is the (Călugăreanu-White) self-linking number of V_k ($k = 1, 2$) and $Lk(C_1, C_2)$ is the (Gauss) linking number of C_1 and C_2. Note that if the pair of rings are unlinked (as in our case, cf. Figure 1a), then $Lk(C_1, C_2) = 0$ and (6) can be further simplified to

$$H(V_1, V_2) = \Gamma^2 [SL(V_1) + SL(V_2)] \ . \quad (7)$$

In general the self-linking number SL, can be decomposed into global geometric quantities, and one can show [19, 20] that $SL(V_k) = Wr(C_k) + T(C_k) + N(R_k)$, where writhing number $Wr(C_k)$, total torsion $T(C_k)$ and intrinsic twist $N(R_k)$ are quantities that depend solely on the shape of the vortex centerline C_k and ribbon R_k (for definitions see [13, 18] and Sec. III here below).

II. NUMERICS AND INITIAL CONDITIONS

The numerical code used for the simulation is described in [4]. It is based on a second-order Strang splitting method in time, and Fourier decomposition in space. Hence, boundary conditions must be periodic; for non-periodic directions the computational domain is doubled and "mirror" vortex rings are introduced in the doubled domain, as was done in [21]. The method conserves mass exactly.

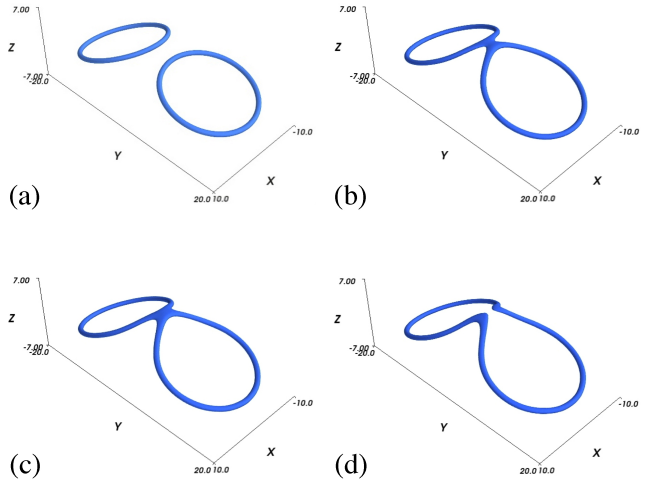

FIG. 1. Time-evolution of interaction and reconnection of two quantum vortex rings; isosurfaces of $\rho = 0.06$. (a) $t = 0$, (b) $t = 10$, (c) reconnection time $t = t^* = 11.81$, $t = 14$.

Initial conditions.—A pair of vortex rings is set at the center of the numerical box. While this particular setting provides a good comparative test for the physics of vortex reconnection [22], it helps to avoid difficulties associated with the numerical implementation of boundary conditions and the topological complexity implied by periodic conditions, while offering a realistic match to simulate the event studied in [14].

At time $t = 0$ the two rings are centered in $(0; \pm 10; 0)$, have radius $R_0 = 8$ and are mutually inclined by an angle $\alpha = \pm\pi/10$ with respect to the horizontal plane (see Figure 1a). The computational domain is $[-20; 20] \times [-30; 30] \times [-20; 20]$. In order to have fine spatial and temporal resolution of the vortex core and of the reconnection process, we have used $\Delta x = \Delta y = \Delta z = \xi/6$ (i.e. the number of points is $240 \times 360 \times 240$) and $\Delta t = 1/80 = 0.0125$.

At each point Q on the vortex ring we place a Frenet triad $\{\hat{\mathbf{t}}, \hat{\mathbf{n}}, \hat{\mathbf{b}}\}$ given by the local unit tangent, normal and binormal to the vortex centerline (no inflexion points emerge during the simulation). For each grid point P in the numerical domain we seek the nearest point Q on the vortex line so that $\overrightarrow{QP}$ identifies the distance of P from the vortex. Thus, $\overrightarrow{QP}$ is locally orthogonal to the vortex, in the plane defined by $\hat{\mathbf{n}}$ and $\hat{\mathbf{b}}$ at Q. In this plane P has polar coordinates (r, θ) centred on Q, where $r = \overline{QP}$ and θ is the angle between $\overrightarrow{QP}$ and $\hat{\mathbf{n}}$.

Each vortex contributes to the initial condition with a density distribution ρ_{0k} given by the Padé approximation [23] $\rho_{0k} = \left(\frac{11}{32} r^2 + \frac{11}{384} r^4\right) / \left(1 + \frac{1}{3} r^2 + \frac{11}{384} r^4\right)$, and phase distribution θ_{0k}. The initial condition due to the presence of both rings is thus $\psi_0 = \sqrt{\rho_{01} \rho_{02}} \exp\left[\mathrm{i}\,(\theta_{01} + \theta_{02})\right]$.

III. EXTRACTION OF GEOMETRIC AND TOPOLOGICAL QUANTITIES

Normalized total length L/ξ, writhe Wr, normalized total torsion T and intrinsic twist N are the global geometric quantities we want to monitor during reconnection. The total twist is given by $Tw = T + N$, and together with Wr gives the self-linking number $SL = Wr + Tw$, a topological invariant. These quantities are well-defined (assuming everything sufficiently smooth) for each individual vortex ring.

The writhe $Wr = Wr(C)$ is analytically defined by

$$Wr = \frac{1}{4\pi} \int_C \int_C \frac{\mathbf{x} - \mathbf{x}^*}{\|\mathbf{x} - \mathbf{x}^*\|^3} \cdot (\, \mathrm{d}\mathbf{x} \times \mathrm{d}\mathbf{r}^*) \ . \qquad (8)$$

where C is the vortex centerline and $\mathbf{x}$ and $\mathbf{x}^*$ denote the position vectors of two points on C.

The normalized total torsion $T = T(C)$ is given by

$$T = \frac{1}{2\pi} \int_C \tau(s)\, \mathrm{d}s \qquad (9)$$

where (from its basic definition) the local torsion $\tau(s)$, function of arc-length s on C, involves third order derivatives of the position vector $\mathbf{x}$ of any point on C.

Intrinsic twist $N = N(R)$ measures the rotation around C of a reference ribbon R (with baseline C) as we move along C. Here R has edges given by C and C', a second curve obtained by translating C a small distance ϵ (the width of R) along a unit normal vector $\hat{\mathbf{u}}$ to C. ϵ is chosen to be constant along C and sufficiently small compared to the local radius of curvature. Clearly R depends on the choice of $\hat{\mathbf{u}}$ and in absence of inflection points, this is always well-defined [17, 18]. If $\varphi(s)$ denotes the angle between $\hat{\mathbf{u}}$ and $\hat{\mathbf{n}}$, we have

$$N = \frac{1}{2\pi} \int_C \frac{\mathrm{d}\varphi(s)}{\mathrm{d}s}\, \mathrm{d}s = \frac{[\Phi]_C}{2\pi} \qquad (10)$$

that measures the number of full rotations of the ribbon R, after one full turn along C. From the definition of total twist one can show [18] that indeed $Tw = T + N$.

IV. RESULTS

Vortex centerlines are extracted from numerical data, first by isolating the tubes whose density $\rho < 0.2$, and then by looking for minima of $\rho/|\boldsymbol{\omega}|$ (minima of density correspond to maxima of vorticity). Particular care has been put to the extraction of sufficiently smooth data. Intrinsic twist is obtained from phase information. The ribbon R is thus obtained by requiring constant phase $\theta = \bar{\theta}$ along C, and by setting $\epsilon = 0.3$, a good compromise between visualization needs and misleading effects. As usual, smoothing was applied to ensure sufficient regularity.

Figure 1 shows four snapshots of the time-evolution of interaction and reconnection of the quantum vortex rings

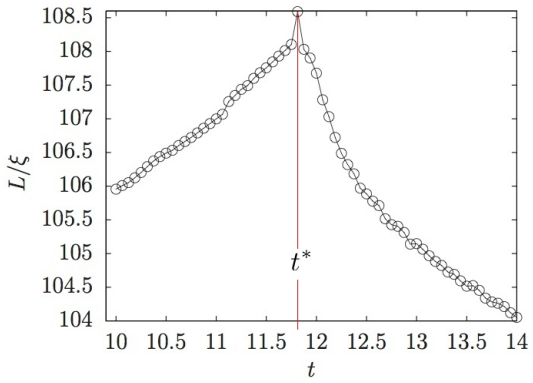

FIG. 2. Normalized total length L/ξ, plotted against time t. The peak in L/ξ is taken as signature of the reconnection time at $t = t^* = 11.81$.

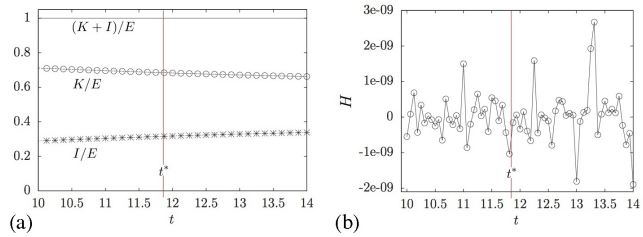

FIG. 3. (a) Normalized total energy (hamiltonian) $(K + I)/E$, normalized kinetic energy K/E and normalized interaction energy I/E plotted against time t. (b) Kinetic helicity H plotted against time t. The vertical line (red online) denotes the reconnection time $t = t^* = 11.81$.

(isosurfaces of $\rho = 0.06$). Before reconnection, the two vortex rings move toward each other, bending upwards in the region near the reconnection site, the more distant parts of the vortices remaining almost un-affected. The change of normalized total length L/ξ of the pair of rings against time is used to check the reconnection process and to the detect reconnection time. The plot is shown in Figure 2 for $t \in (10, 14)$. The marked peak at $t = t^* = 11.81$, after stretching, is taken as signature of the reconnection time. The maximum value $L_{\max} \approx 108.6\,\xi$ corresponds to about 8% of increase with respect to the initial total length, given by $L_0 \approx 100.5\,\xi$. For $t > t^*$ the system relaxes at a faster rate, confirming the time asymmetry found in earlier work [4].

As a further check, we plot the hamiltonian (E) given by the normalized total energy $(K+I)/E$ and, separately, the normalized kinetic energy K/E and interaction energy I/E, given by (4) (see Figure 3a). Kinetic helicity is computed according to eq. (5). As shown in Figure 3b its value remains bounded, i.e. $|H| < 10^{-9}$, that is approximately zero throughout the reconnection process (at these length scales the spikes of the plot in Figure 3b are essentially due to numerical noise). A check on vortex strength confirms the conservation of Γ before and after reconnection. A close-up view of the vortex centerlines (in red, online) and reference ribbons (green and blue, on-

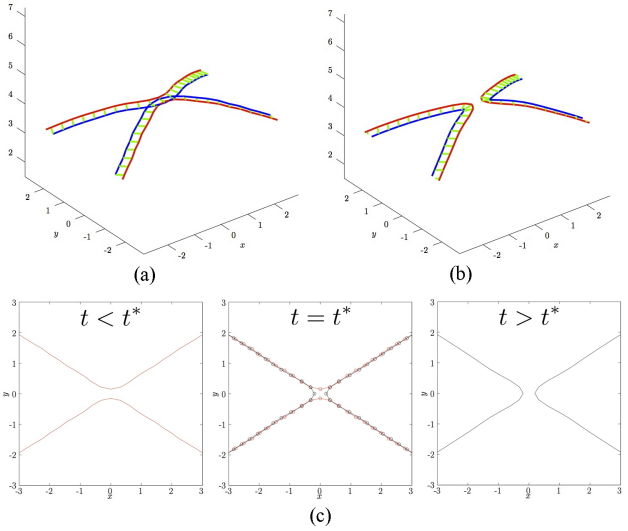

FIG. 4. A close-up view of the vortex centerlines (red online) and reference ribbons (green and blue online, otherwise pale grey and darker) (a) immediately before reconnection at $t = 11.81$, and (b) immediately after reconnection at $t = 11.88$. The transition is shown at maximum numerical resolution: (c) vortex centrelines just before (red online) and after (black) reconnection; the state in-between (at $t = t^*$) shows that reconnection is numerically triggered by a jump at just two nodal points (circles).

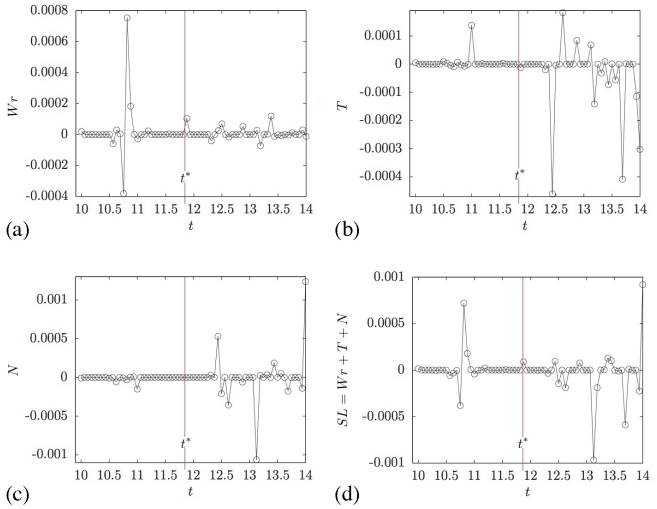

FIG. 5. (a) Writhe Wr, (b) normalized total torsion T, (c) normalized intrinsic twist N (with $\bar{\theta} \approx 50°$) and self-linking number SL plotted against time t. The vertical line (red online) denotes the reconnection time $t = t^* = 11.81$.

line) immediately before and after reconnection is shown in the plots of Figure 4a,b. The reconnection event takes place at a much faster timescale, well beyond numerical accuracy. To monitor as close as possible the topological transition, the event is represented at maximum numerical resolution by showing the diagrams of the discretized vortex centrelines in Figure 5c. As we can see from the central diagram of Figure 5c (at $t = t^*$) the reconnecting event is numerically triggered by a jump at the two nodal points (circles) of closest approach, demonstrating that in the limit of numerical resolution reconnection involves only the mutual cancellation of two anti-parallel polygonal segments.

Finally, we examine the individual contributions to the self-linking number by using the independent equations (8)–(10). Plots of Wr, T, N and SL against time are shown in Figure 5. The ribbon R is found to be $\theta = \bar{\theta} \approx 50°$. Writhe and twist remain very small throughout the process. They are identically zero only at $t = 0$, when the vortex rings are exactly planar tori, whereas for $t > 0$ the vortex centerlines become gradually deformed. Except for a few spikes, which are not related to reconnection, $|Wr| < 10^{-4}$ and $|Tw| < 2 \times 10^{-4}$. Numerical errors associated to the computation of Tw are generally larger than those on Wr, because of the higher-order derivatives involved in the computation of the normalized total torsion (see Figure 5b) and the additional numerical noise associated with the computation of N (see Figure 5c). The numerical code has been validated by computing Wr and Tw of known benchmarks, and we are confident that the reported spikes are only due to accumulation of numerical errors. Thus, we conclude that all plots of Figure 5 show consistently $Wr = T = N = SL = 0$ throughout the reconnection process.

V. CONCLUSIONS

We have performed numerical simulations of the GPE, that resolve the fine structure of the vortex-core under anti-parallel reconnection of the tube strands of two colliding quantum vortex rings. This simple scenario provides a good benchmark for comparison with earlier works on direct numerical simulation of reconnecting vortex rings under Navier-Stokes equations [24, 25], and an ideal setup for clarifying recent contradictory results obtained by experiments and theoretical modeling on classical vortex dynamics.

Reconnection under Gross-Pitaevskii is clearly manifested by the generation of a peak in total length, and this is taken as a marker of the reconnection event. We took extra care to monitor the behaviour of several geometric quantities during reconnection. As predicted by geometric analysis [13] writhe and total torsion are found to remain conserved, whereas there is no change in total intrinsic twist, all this keeping clearly self-linking number invariant. Self-helicity, computed independently by using eq. (5), is found consistently to remain conserved during reconnection. Since in our experiment the (Gauss) linking number Lk is always zero (the rings remain unlinked throughout the process), there is no contradiction with the fact that during reconnection topology actually changes (as indeed happens here). The fact that self-helicity, and hence total helicity, remains conserved

during reconnection is thus something not only new for quantum systems, but also in good agreement with the recent experimental observations of reconnecting vortices in water [12]. The methods used here can certainly be extended to study more complex topologies and further work is indeed in progress to analyze and to extend this preliminary findings.

[1] S. Kida and M. Takaoka, Annu. Rev. Fluid Mech. **26**, 169 (1994).
[2] A.K.M.F. Hussain and K. Duraisamy, Phys. Fluids **23**, 021701 (2011).
[3] M.S. Paoletti *et al.*, Physica D **239**, 1367 (2010).
[4] S. Zuccher, *et al.*, Phys. Fluids **24**, 125108 (2012).
[5] Y.T. Lau, and J.M. Finn, Phys. Plasmas **3**, 3983 (1996).
[6] E. Priest and T. Forbes, Magnetic Reconnection, Cambridge University Press (2000).
[7] S. Lugomer, J. Fluids & Structures **13**, 647 (1999).
[8] A.V. Vologodskii *et al.*, J. Mol. Biol. **278**, 1 (1998).
[9] W.F. Vinen, Phil. Trans. R. Soc. A **366**, 2925 (2008).
[10] C.F. Barenghi *et al.*, Proc. Natl. Acad. Sci. USA **111**, 4647 (2104).
[11] R.M. Kerr, Phys. Rev. Lett. **106**, 224501 (2011).
[12] M.W. Scheeler *et al.*, Proc. Natl. Acad. Sci. USA **111**, 4647 (2014).
[13] C.E. Laing *et al.*, Sci. Rep. **5**, 9224 (2015).
[14] Y. Kimura and H.K. Moffatt, J. Fluid Mech. **751**, 329 (2014).
[15] P.G. Saffman, Vortex Dynamics, Cambridge University Press (1992).
[16] H.K. Moffatt, J.Fluid Mech. **35**, 117 (1969).
[17] R.L. Ricca and H.K. Moffatt, in *Topological Aspects of the Dynamics of Fluids and Plasmas* [H.K. Moffatt *et al.* (ed.)] p. 225, Kluwer Acad. Publs. (1992).
[18] H.K. Moffatt and R.L. Ricca, Proc. R. Soc. Lond. A **439**, 411 (1992).
[19] G. Călugareănu, Czech. Math. J. **11**, 588 (1961).
[20] J.H. White, Am. J. Math. **91**, 693 (1969).
[21] J. Koplik and H. Levine, Phys. Fluids **71**, 1375 (1993).
[22] P.M. Walmsley *et al.*, Phys. Rev. Lett. **113**, 125302 (2014).
[23] N.G. Berloff, J. Phys. A: Math. Gen. **37**, 1617 (2004).
[24] S. Kida, M. Takaoka and F. Hussain, Phys. Fluids A **1**, 630 (1989).
[25] P Chatelain, D Kivotides and A Leonard, Phys. Rev. Lett. **90**, 054501 (2003).